ORIGINAL ARTICLE

Bone morphogenetic protein-7 is a MYC target with prosurvival functions in childhood medulloblastoma

G Fiaschetti[1], D Castelletti[1], S Zoller[2], A Schramm[3], C Schroeder[4], M Nagaishi[5], D Stearns[6], M Mittelbronn[7], A Eggert[3], F Westermann[4], H Ohgaki[5], T Shalaby[1], M Pruschy[8], A Arcaro[9] and MA Grotzer[1]

[1]Department of Oncology, University Children's Hospital, Zurich, Switzerland; [2]Functional Genomics Center Zurich, UZH/ETH, Zurich, Switzerland; [3]Division of Hematology/Oncology, University Children's Hospital Essen, Essen, Germany; [4]Department Tumor Genetics, German Cancer Research Center (DKFZ), Heidelberg, Germany; [5]Section of Molecular Pathology, International Agency for Research on Cancer, World Health Organization, Lyon, France; [6]Department of Pathology, Johns Hopkins University, Baltimore, MD, USA; [7]Institute of Neurology (Edinger Institute) Goethe-University Frankfurt, Frankfurt/Main, Germany; [8]Department Radiation Oncology, University Hospital, Zurich, Switzerland and [9]Division of Pediatric Hematology/Oncology, Department of Clinical Research, University of Bern, Bern, Switzerland

Medulloblastoma (MB) is the most common malignant brain tumor in children. It is known that overexpression and/or amplification of the MYC oncogene is associated with poor clinical outcome, but the molecular mechanisms and the MYC downstream effectors in MB remain still elusive. Besides contributing to elucidate how progression of MB takes place, most importantly, the identification of novel MYC-target genes will suggest novel candidates for targeted therapy in MB. A group of 209 MYC-responsive genes was obtained from a complementary DNA microarray analysis of a MB-derived cell line, following MYC overexpression and silencing. Among the MYC-responsive genes, we identified the members of the bone morphogenetic protein (BMP) signaling pathway, which have a crucial role during the development of the cerebellum. In particular, the gene *BMP7* was identified as a direct target of MYC. A positive correlation between MYC and BMP7 expression was documented by analyzing two distinct sets of primary MB samples. Functional studies *in vitro* using a small-molecule inhibitor of the BMP/SMAD signaling pathway reproduced the effect of the small interfering RNA-mediated silencing of *BMP7*. Both approaches led to a block of proliferation in a panel of MB cells and to inhibition of SMAD phosphorylation. Altogether, our findings indicate that high MYC levels drive *BMP7* overexpression, promoting cell survival in MB cells. This observation suggests the potential relevance of targeting the BMP/SMAD pathway as a novel therapeutic approach for the treatment of childhood MB.
Oncogene (2011) **0,** 000–000. doi:10.1038/onc.2011.10

Keywords: BMP7; MYC; medulloblastoma; brain tumor; pediatric cancer

Correspondence: Professor Dr MA Grotzer, Department of Oncology, University Children's Hospital, Steinwiesstrasse 75, Zurich CH-8032, Switzerland.
E-mail: Michael.Grotzer@kispi.uzh.ch

Introduction

Medulloblastoma (MB) represents >20% of all pediatric tumors of the central nervous system (Gurney and Kadan-Lottick, 2001), and is characterized by aggressive clinical behavior and high risk of leptomeningeal dissemination (Engelhard and Corsten, 2005). Multimodal therapy (surgery, radiotherapy and chemotherapy) has improved the overall survival rate. However, about 30% of patients are still incurable, and survivors often suffer from severe tumor- and therapy-related cognitive and neurological dysfunctions (Mulhern *et al.*, 2005). MB can be subdivided into different histological variants (Eberhart *et al.*, 2002; Lamont *et al.*, 2004); the large-cell/anaplastic MB (20–25% of patients) represents the most aggressive subtype, and is associated with a high degree of genomic instability and deregulated expression of the oncogene *MYC* (Stearns *et al.*, 2006; Gilbertson and Ellison, 2008).

MYC represents a family of pleiotropic transcription factors that activate/repress a large group of target genes (Grandori *et al.*, 2000; Adhikary and Eilers, 2005) that are, in turn, the effectors of MYC-dependent biological responses, ranging from cell growth, proliferation and migration to programmed cell death and differentiation. MYC is primarily expressed during development and is mainly repressed in adult tissues, in which aberrant expression (upregulation) can drive neoplastic transformation (Littlewood and Evan, 1990). In MB, MYC upregulation can originate from genomic amplification (4–10% of MB patients; Neben *et al.*, 2004) or mRNA overexpression (30–65% of patients; Herms *et al.*, 2000; Aldosari *et al.*, 2002), and it can occur as a downstream effect of deregulated signaling pathways (Guessous *et al.*, 2008) that are involved in the development of granule neuron precursor cells (GNPs) of the cerebellum (Gilbertson and Ellison, 2008).

Different approaches have been evaluated to target MYC in various malignancies, including MB (Vita and Henriksson, 2006; Grotzer *et al.*, 2009). However, direct pharmacological targeting of transcription factors has

proven difficult, thus warranting the effort of investigating in more detail genes that are downstream of MYC as novel therapeutic targets. Furthermore, a selective targeting of downstream effectors would aim at preserving the anti-proliferation (for example pro-apoptotic) functions of MYC.

In this study, we combined gene expression data from MB-derived cell lines, which had been engineered to either overexpress or silence *MYC*. Among the MYC-responsive genes, we searched for candidate drivers of MYC-dependent tumorigenesis in MB. The results suggested the possible relevance of bone morphogenetic proteins (BMPs), which are cytokines of the family of the transforming growth factor-β (Blanco Calvo *et al.*, 2009). BMPs can be activated, both in a paracrine and autocrine way, to promote recruitment of cell surface serine/threonine kinase receptors, thus triggering activation of SMAD transcription factors (Miyazono *et al.*, 2005, 2010).

Many studies report on alterations of the BMP pathway in several tumor systems, including breast, prostate, lung, and colon cancers, as well as glioblastoma, osteosarcoma and MB (Arihiro and Inai, 2001; Langenfeld *et al.*, 2003; Miyazaki *et al.*, 2004; Raida *et al.*, 2005; Piccirillo and Vescovi, 2006; Ye *et al.*, 2007; Buijs *et al.*, 2007a; Dai *et al.*, 2008). Similar to other transforming growth factor-β members (Derynck *et al.*, 2001), BMPs may have a dual role in cancer, both promoting and repressing tumorigenesis in several models (Buijs *et al.*, 2007a, b; Ye *et al.*, 2009; Thawani *et al.*, 2010). BMP7, for instance, was shown to promote migration and invasion of prostate cancer cells (Feeley *et al.*, 2005), but also to inhibit prostate tumor cell growth *in vivo* (Buijs *et al.*, 2007b). Miyazaki *et al.* (2004) showed a dose-dependent effect of BMP7, which inhibited proliferation of androgen-insensitive prostate cells at high concentrations, whereas low doses had a pro-proliferative effect. In breast cancer, the expression level of *BMP7* was found inversely correlated to tumorigenicity and invasiveness *in vitro* (Buijs *et al.*, 2007a), but it was also found to cause abnormal proliferation in p53-deficent breast cancer cells when knocked down (Yan and Chen, 2007). Although apparently contradictory, these data reflect the complexity of the BMP/SMAD signaling pathway (Ye *et al.*, 2009), leading to diverse heterogeneous cellular responses, which can be tissue- and cell type-specific and result from the cross-talk with the microenvironment. This latter heavily influences the temporal and spatial expression of BMPs (Sieber *et al.*, 2009), implying also that co-expression of antagonists (Walsh *et al.*, 2010; Yanagita, 2005) or modulators (Balemans and Van Hul, 2002; Yanagita, 2009), as well as the activation status of other pathways (Miyazono *et al.*, 2005; Guo and Wang, 2009), all contribute significantly to the diverse responses observed.

Finally, because of the relevance of BMPs during cerebellum development (by regulating proliferation, cell cycle exit, migration and differentiation of GNPs; Gilbertson and Ellison, 2008), it is not surprising that BMPs are likely to have a role in tumorigenesis and at least in a subset of MB tumors (Thompson *et al.*, 2006; Grimmer and Weiss, 2008; Behesti and Marino, 2009; Sutter *et al.*, 2010). In this respect, our experimental results are consistent with this biological hypothesis and provide an important contribution by linking, for the first time, a BMP family member to the oncogene MYC, in the context of MYC-dependent prosurvival mechanisms in MB.

Results

Identification of MYC-responsive genes in a model of MB
To identify MYC-driven tumorigenic functions in MB, DAOY and DAOY-derived cells were genetically manipulated to either enhance or silence *MYC* expression (Stearns *et al.*, 2006), and their expression profiles were analyzed by cDNA microarray. In one set of experiments, we evaluated the transcriptional changes induced by *MYC* upregulation in DAOY cells by comparing the profiles of two *MYC*-overexpressing clones (DAOY M2.1 and M14) with those of wild-type DAOY and empty-vector-transfected DAOY V11 cells. The two clones shared 98% similarity in differentially expressed genes, they were substantially identical in terms of transcriptional changes associated with *MYC* expression on the genetic background of DAOY cells. The lists of genes associated with *MYC* overexpression in DAOY M2.1 and M14 cells were intersected to select only common genes and corrected for the contribution of the empty vector. This analysis enabled us to define a list of genes associated with *MYC* overexpression. In addition, we analyzed the transcriptome of DAOY M2.1 cells transfected with *MYC*-specific small interfering RNA (siRNA) normalized to control/non-targeting siRNA and found a group of genes associated with *MYC* knockdown. In this latter set of experiments, the expression analysis was carried out at 48 h post transfection. This time point was chosen because it showed the most efficient downregulation of *MYC* and of its known direct target telomerase reverse transcriptase (*TERT*) (Supplementary Figure S1A). Figure 1 shows the variation of MYC in all cell lines in the study, at both the mRNA (Figure 1a) and protein (Figure 1b) levels.

To select only those entities up/downregulated in a consistent manner in both sets of experiments, we intersected the two lists of genes. We obtained a group of 209 genes that were responsive to *MYC* gene modulation with absolute fold change $\geqslant 2.0$ and *P*-value < 0.01 (Figure 1c). Of the 209 genes, 105 were

Figure 1 Gene expression analysis. (**a**) The mRNA expression levels of *MYC* were quantified by quantitative real-time PCR in DAOY cells and in DAOY-derived cell clones (empty-vector-transfected DAOY V11, *MYC*-transfected DAOY M2.1 and M14). Data are normalized to *SDHA* and to MYC expression in normal human cerebellum (defined as 1). (**b**) MYC protein levels were evaluated by immunoblotting and compared with β-tubulin as the loading control (ctrl). (**c**) Heat map representing the 209 MYC-responsive genes.
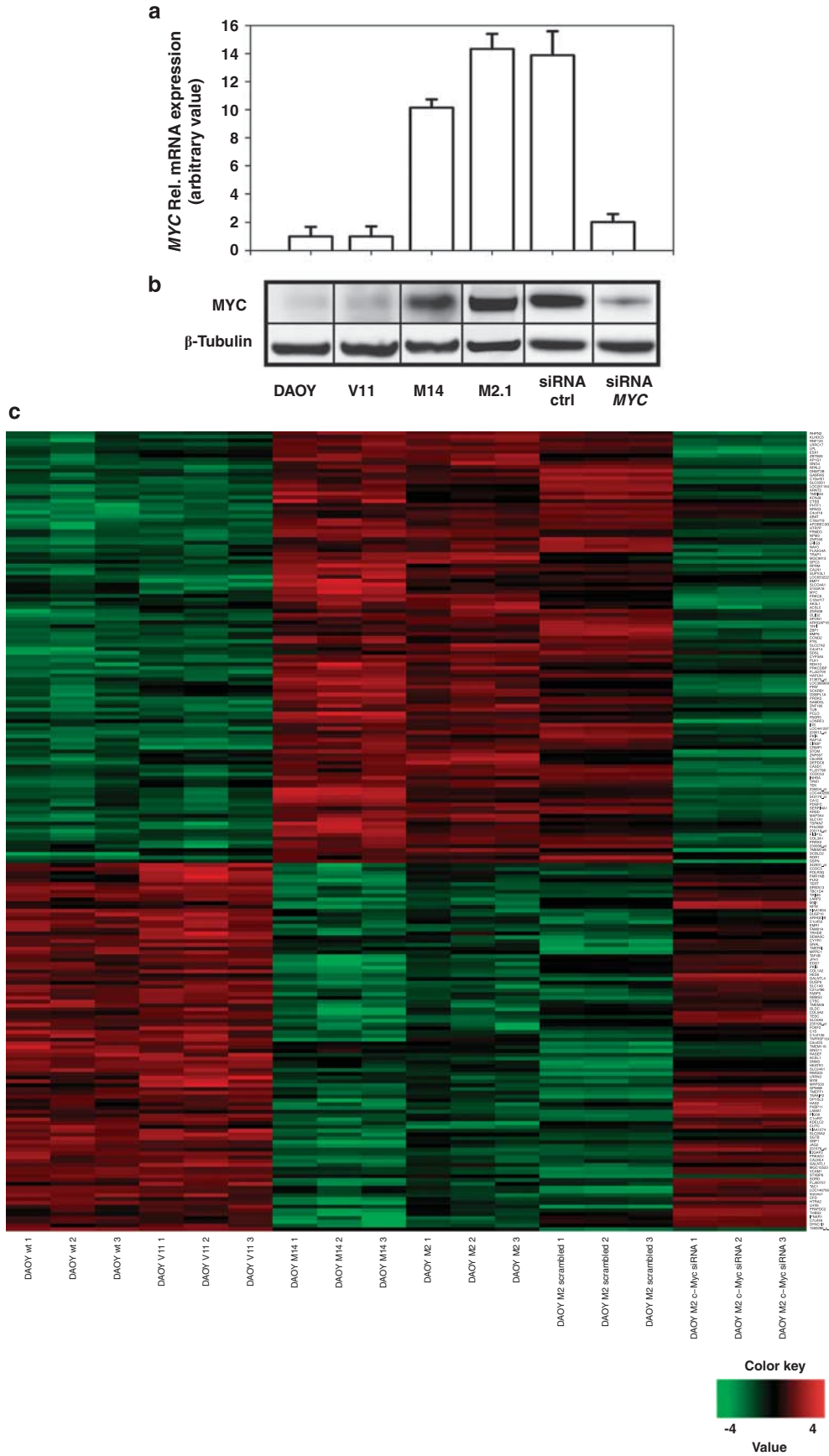
a

b

c

Table 1 Differential expression of BMPs and BMPR-I/II as obtained by the cDNA microarray analysis of DAOY-derived cells

Gene name	Description	M2-high MYC versus ctrl		M14-high MYC versus ctrl		MYC silenced versus ctrl	
		FC	P-value	FC	P-value	FC	P-value
Ligands							
BMP2	Bone morphogenetic protein 2	1.99	0.0022	2.78	0.00056	−1.42	0.0029
BMP4	Bone morphogenetic protein 4	−1.68	0.0035	−1.17	0.33	1.61	0.00096
BMP6	Bone morphogenetic protein 6	9.40	0.0002	14.83	0.0000072	−1.71	0.00005.8
BMP7	Bone morphogenetic protein 7 (osteogenic protein 1)	2.13	0.00037	8.67	0.00004.6	−2.58	0.000001.4
Receptors							
BMPR1A	Bone morphogenetic protein receptor, type IA	−1.16	0.26	−1.11	0.72	1.47	0.00047
BMPR2	Bone morphogenetic protein receptor, type II	1.41	0.0006	−1.25	0.27	1.22	0.0095
ACVR1	Activin A receptor, type I	−1.03	0.25	1.16	0.35	2.26	0.00005.8
ACVR1B	Activin A receptor, type 2 B	−1.12	0.031	2.28	0.00072	−1.61	0.0011
ACVR2A	Activin A receptor, type IIA	−1.23	0.03	1.29	0.17	−1.57	0.00033
ACVR2B	Activin A receptor, type IIB	−1.04	0.56	1.93	0.0005	−2.15	0.00026
Pseudoreceptors							
BAMBI	BMP and activin membrane-bound inhibitor homolog	1.18	0.52	1.13	0.39	2.91	0.0000004.1
Ligand inhibitors							
GPC3	Glypican 3	2.29	0.00075	2.79	0.0042	−1.69	0.00023
Secretory antagonist							
CRIM1	Cysteine rich transmembrane BMP regulator 1 (chordin-like)	−1.21	0.22	−1.49	0.017	1.58	0.00086

Abbreviations: BMPs, bone morphogenetic proteins; BMPR, BMP receptor; cDNA, complementary DNA; ctrl, control; FC, fold change. Ctrl, DAOY/DAOY V11; M2/M14, DAOY M2.1/M14 clones; MYC silenced, DAOY M2.1 transfected with *MYC*-small inhibitory RNA.

upregulated and 104 downregulated on ectopic expression of *MYC* (Supplementary Table 1). This group of genes was analyzed by using different bioinformatics tools, such as GeneGO MetaCore, that allowed us to draw functional networks between genes based on the literature.

Our experimental data included several known direct targets of MYC, such as *CCND2* (Adhikary and Eilers, 2005) and *TERT* (Wu *et al.*, 1999), which overlapped with the MYC-target gene database (www.myccancer-gene.org/site/mycTargetDB.asp). In fact, overexpression of *MYC* increased the *CCND2* level by 3.1- and 2.3-fold in DAOY M2.1 and M14 cells, respectively, whereas *MYC* silencing repressed the same gene by 8.4-fold. In contrast, a gene that is known to be negatively regulated by MYC, inhibin-β A (*INHBA*), was significantly downregulated in DAOY M2.1 and in DAOY M14 cells (3.8- and 3.7-fold change, respectively) and upregulated on *MYC* silencing (3.9-fold change). The cDNA microarray data were validated by quantifying the mRNA expression level of a group of representative MYC-target genes. The expression changes of *TERT* and *CCND2* following both upregulation (Supplementary Figure S1B) and silencing of *MYC* (Supplementary Figure S1C) are reported. As a negative control, the expression of cyclin A2 (*CCNA2*), which is not a target of MYC, was analyzed (Supplementary Figure S1A,B).

Effect of MYC modulation on components of the BMP pathway
Growing evidence suggests the functional relevance of BMPs in the onset of a subset of MB tumors, which is currently attributed to abnormal development of GNP cells of the external granular layer of the cerebellum (Marino, 2005; Crawford *et al.*, 2007; Gilbertson and Ellison, 2008; Sutter *et al.*, 2010). Interestingly, several members of the BMP pathway were differentially expressed following overexpression or silencing of *MYC* (Table 1), suggesting a regulatory effect of MYC on this pathway in MB.

In particular, a general increase in the mRNA expression levels of some BMP ligands (*BMP2, 6* and *7*) in DAOY M2.1 cells hinted at MYC-dependent activation. Moreover, subtypes of BMP receptors (BMPRs) type I-II were also represented, although only a few of them could be validated in our cellular models. Similar to the majority of BMPs, the mRNA level of glypican-3 (*GPC3*), a soluble inhibitor of BMPs (Grisaru *et al.*, 2001; Filmus *et al.*, 2008), increased with *MYC* upregulation, and it may be responsible for a negative-feedback loop on the pathway. Finally, our microarray data did not show significant alteration of members of the SMAD family of transcription factors or of the SMAD-target genes inhibitors of differentiation (*ID*; Miyazono, 1999). This observation would imply the involvement of alternative downstream effectors, not fully characterized yet.

BMP7 as downstream target of MYC in MB
The correlation analysis performed by using GeneGO set a subgroup of the selected 209 *MYC*-responsive genes in direct and functional links with MYC, according to published data (Supplementary Figure S2). In particular, several networks revealed a direct

correlation between *MYC* and *BMP7*, which we studied in more detail, trying to elucidate the MYC-dependent regulation of *BMP7* and the relevance of the BMP pathway in our model of MB. From the gene expression profiling data, *BMP7* was upregulated in *MYC*-over-expressing DAOY M2.1 and M14 cells (2.1- and 8.7-fold change, respectively), whereas *BMP7* was repressed in cells silenced for *MYC* (2.6-fold change; Table 1). Another BMP member, *BMP6*, was found strongly upregulated on *MYC* overexpression (9.4-fold change). However, on *MYC* silencing, the transcriptional level of *BMP6* did not consistently correlate with *MYC* levels (1.7-fold-change; Table 1).

To demonstrate that the MYC transcription factor regulates transcription of *BMP7*, the ability of MYC to bind the promoter of *BMP7* was evaluated by chromatin immunoprecipitation (ChIP), performed in different MB cell lines. Genomic DNA was extracted and precipitated with a MYC-specific antibody to enrich for MYC-binding promoter sequences, which were hybridized to a promoter oligo array (Ma *et al.*, 2010). We observed an enrichment of DNA fragments surrounding the transcriptional start site of *BMP7*, including regions that contain canonical binding sites for MYC (Figure 2), demonstrating that MYC can

Figure 2 Binding of MYC to the *BMP7* promoter in MB cells. ChIP-on-chip data show occupancy of the *BMP7* genomic sequence by MYC in D487 and D283 medulloblastoma cells, respectively. The genomic positions for probes and their enrichment ratios are given for MYC at the *BMP7* locus in D487 and D283 cells. The horizontal line indicates the median enrichment ratio for MYC versus input as calculated from all probes for chromosome 20.

regulate the expression of *BMP7* by binding the *BMP7* promoter.

BMP7 is expressed in MB tumor samples and correlates with MYC expression

A total of 66 samples of MB available as a tissue microarray (TMA) were probed for BMP7 immuno-reactivity. Cytoplasmic expression of BMP7 was quantified as positive in 10–50% cells in 17 tumors (26% MBs), as 51–90% cells in 16 tumors (24% MBs) and as >90% cells in 14 tumors (21% MBs), whereas 19 tumors (29%) expressed no BMP7 (Figure 3a and b). Notably, BMP7 could not be detected in any of the 16 normal cerebellum cores (Figure 3c). Normal human renal tubule cells were used as a positive control, as they express high levels BMP7 in the cytosol (Figure 3d).

To find a possible correlation between *BMP7* and *MYC* in primary MBs, the mRNA expression levels of both genes were determined in 38 MB samples from the TMA. The results clearly indicated a positive correlation between *BMP7* and *MYC* (Pearson's correlation value = 0.42; *P*-value = 0.0095; Figure 3e). The observation that *BMP7* and *MYC* positively correlate in primary tumors was confirmed by the unsupervised analysis of a different set of gene expression data, obtained from 46 MBs previously published by Thompson *et al.* (2006; Supplementary Figure S3). Although this analysis showed the correlation of *BMP7* with *MYC* expression in primary tumors, no significant correlation was found between *MYC* and other BMP members (from Table 1).

MYC-dependent expression of BMP7 and SMAD1/5/8 activation in MB cells

The MYC-dependent expression of *BMP7* was validated in different cell lines (Figure 4). *MYC* overexpression significantly increases the mRNA level of *BMP7* (Figure 4a). On the other hand, *BMP7* was down-regulated in DAOY M2.1 cells transfected with *MYC* siRNA (Figure 4b), similarly to *TERT* that is a known MYC direct target gene (see also Supplementary Figure S1A). Although *BMP6* mRNA increased on *MYC* overexpression, no effect was observed by silencing the oncogene. We could not find a significant correlation between the expression of *BMP6*, *MYC* and *TERT* (Supplementary Figure S1A).

To discriminate between the intracellular and the secreted (active) form of BMP7, both total cell lysates and supernatants were analyzed for BMP7 expression, by immunoblotting (Figure 4c) and enzyme-linked immunosorbent assay (ELISA; Figure 4d), respectively. The results confirmed that the MYC-dependent expression of BMP7 induced also an increase of the BMP7 protein, both in the precursor and the mature secreted form. In fact, BMP7 was detectable in the supernatant only in *MYC*-overexpressing cells, whereas it was undetectable (both in total cell lysates and supernatant) in cells bearing only one *MYC* copy (Figure 4c, left panel). Complementary to this effect, silencing of *MYC*
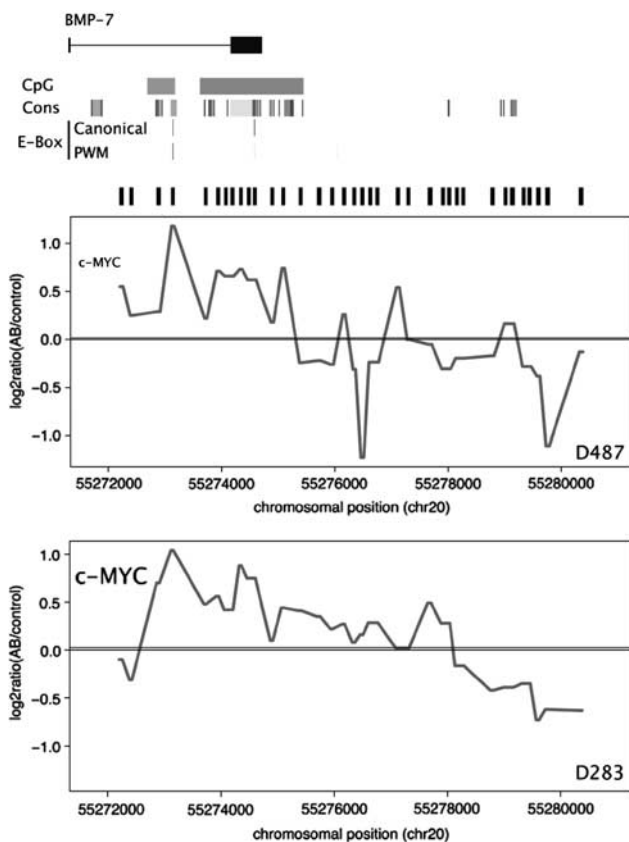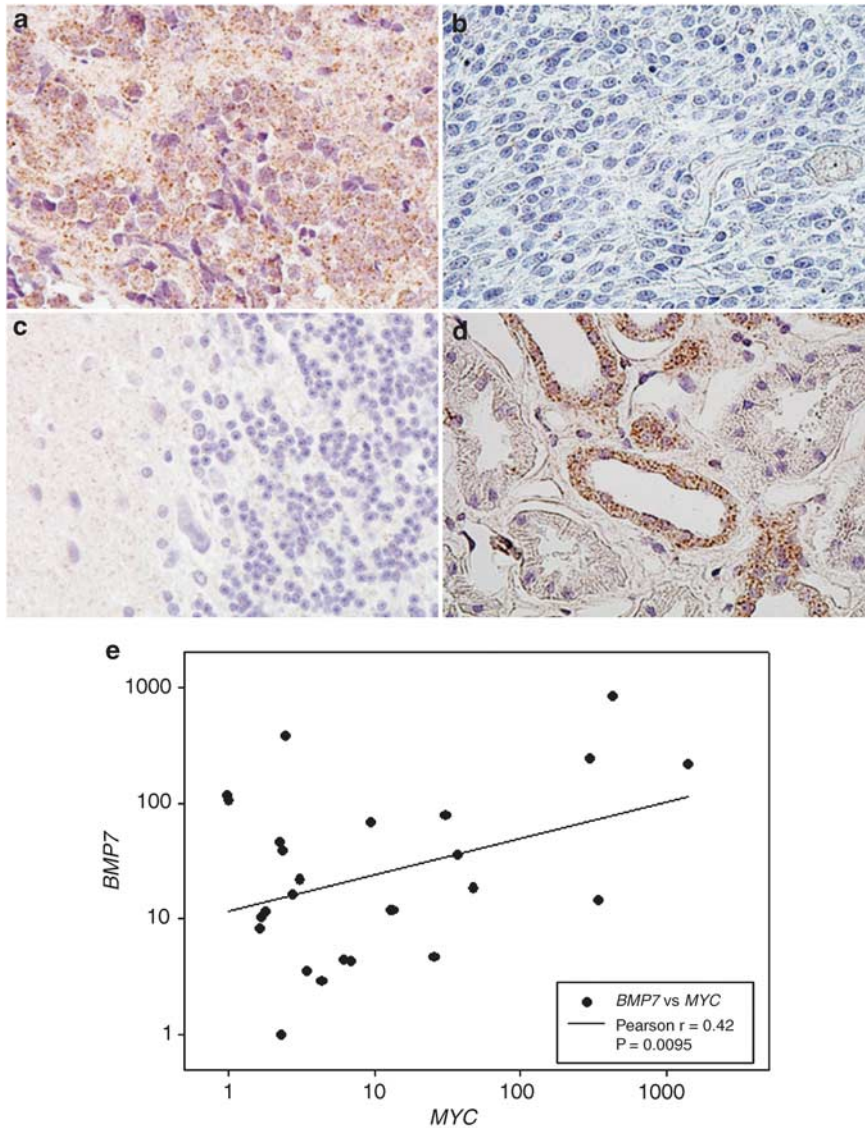
Figure 3 MB TMA analysis and *BMP7/MYC* correlation study in MB patients. (**a**) BMP7 immunohistochemistry showing cytoplasmic expression of BMP7 in the majority of neoplastic cells in MB (case number 97), and (**b**) no expression of BMP7 in a different MB (case number 38). (**c**) Normal cerebellum shows no BMP7 immunoreactivity. (**d**) Renal tubule cells served as a positive control showing cytoplasmic staining for BMP7. (**e**) The mRNA expression level of *BMP7* and *MYC* was evaluated by quantitative real-time PCR in a subset of the MB patient samples present on the TMA. Values were normalized to ribosomal protein 18S and to *BMP7* and *MYC* expression in normal human cerebellum (defined as 1).

caused depletion of BMP7 in cell lysates (Figure 4C, right panel) as well as in the medium (Figure 4e).

Next, we investigated whether MYC-dependent modulation of BMP7 also affected the downstream SMAD signaling pathway. Indeed, the levels of phosphorylated SMAD1/5/8 increased in MYC/BMP7-overexpressing cells, suggesting an enhanced ligand-dependent engagement of the upstream receptors (Figure 4c, left panel). On the other hand, we observed a significant reduction of SMAD1/5/8 phosphorylation in cells that were depleted of MYC (Figure 4c, right panel). As further evidence, we report on a BMP7-dependent increase of active SMAD1/5/8 in DAOY V11 and DAOY M2.1 cells, after addition of recombinant BMP7 to the medium (Figure 4f).

Targeting BMP/SMAD signaling pathway in MB
To investigate the relevance of the BMP/SMAD pathway in MB cells, we evaluated the effect of interfering with SMAD activation by using different approaches. Silencing of *BMP7* in DAOY M2.1 cells was evaluated in a time-course experiment (Figure 5a). Along with the decreased amount of secreted BMP7 in the medium (Figure 5b), BMP7 downregulation induced cell death with concomitant inhibition of cell viability (Figure 5c). These results indicate the functional relevance of BMP7 as an effector of the prosurvival functions of MYC in MB. On silencing, *BMP7* mRNA level decreased by ∼80%, whereas the secreted BMP7 decreased by ∼50%, compared with non-targeting-siRNA-transfected cells. This discrepancy could be explained
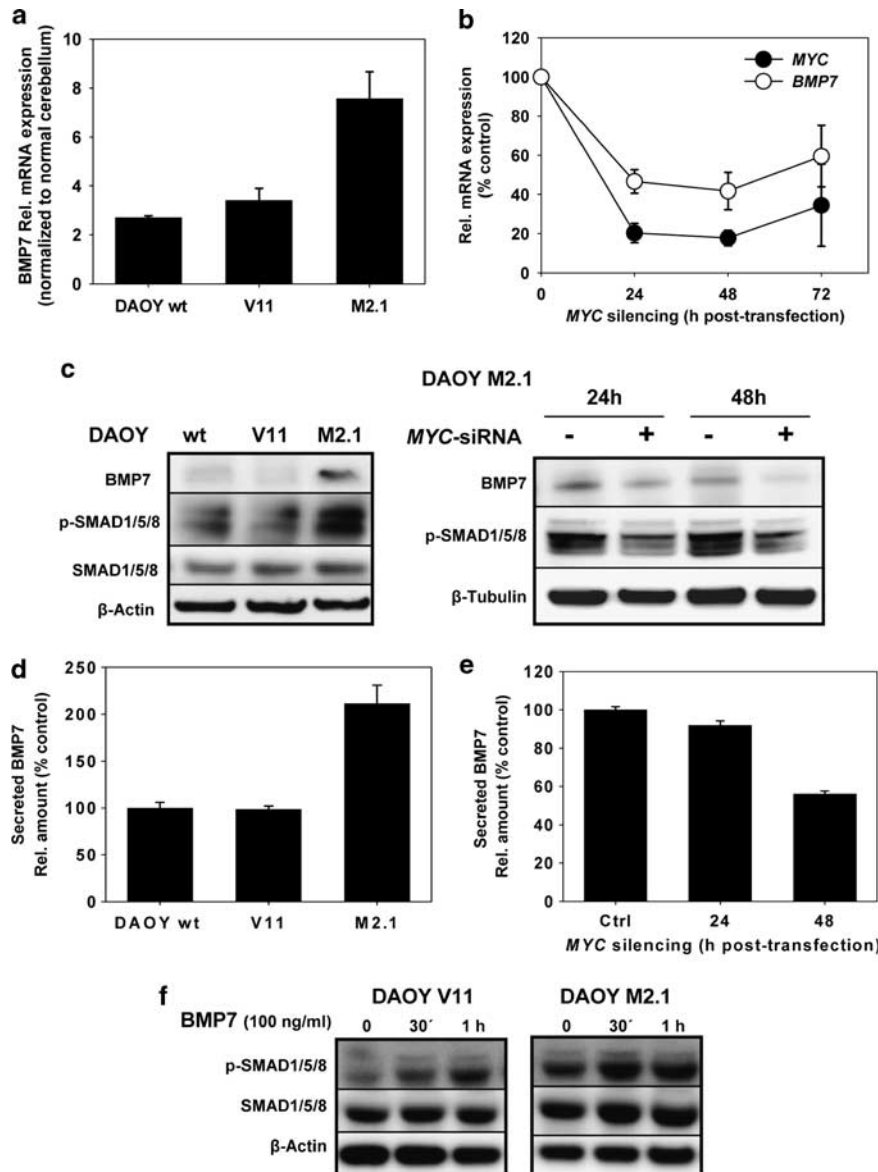
Figure 4 *MYC*-dependent regulation of *BMP7* and SMAD activation. (**a**) *BMP7* mRNA was evaluated by quantitative real-time PCR in the indicated cell lines and reported as relative expression normalized to normal cerebellum (defined as 1). (**b**) *MYC* and *BMP7* mRNA expression levels in DAOY M2.1 cells transfected with *MYC*-siRNA are reported as the percentage of the expression in cells transfected with control/non-targeting siRNA. *SDHA* expression was used for internal normalization. (**c**) Protein levels of BMP7, phospho-SMAD1/5/8, and total SMAD1/5/8 were evaluated by western blot in DAOY cells and DAOY-derived cell clones (left panel) and in DAOY M2.1 cells with *MYC* silenced (right panel). Expression of either β-actin or β-tubulin was detected as control. (**d**, **e**) The relative amount of secreted BMP7 in cell supernatants was evaluated by ELISA following *MYC* upregulation or silencing, respectively. Percentages are in comparison to the BMP7 secreted by DAOY cells (**d**) or by DAOY M2.1 transfected with control siRNA (**e**). (**f**) The activation status of SMAD1/5/8 was also analyzed following cell stimulation with BMP7 100 ng/ml for the indicated durations.

by the documented stability of the *BMP7* mRNA (Guhaniyogi and Brewer, 2001; Buijs *et al.*, 2010), which would justify a higher amount of protein detected than expected. However, we cannot exclude that the cellular responses we observed are associated not only with the downregulation of *BMP7* but also with a more general alteration of the entire BMP network following MYC modulation.

The effect of other BMPs and BMPR isoforms was evaluated by silencing *BMP2*, *BMP6* and all known *BMPR-I/II* receptors, which were found upregulated,

together with *BMP7*, in *MYC*-overexpressing cells. Among the BMPs, downregulation of *BMP6* showed an effect similar to *BMP7* silencing (Supplementary Figure S4A), whereas among the BMPRs only downregulation of *ACVR1* reduced cell viability significantly. Although not considered as direct target of MYC, BMP6 was considered in double-knockout experiments, to prove whether silencing of both *BMP6* and *BMP7* had a more pronounced effect on cell viability than downregulating *BMP7* alone. Single silencing of *BMP6* or *BMP7* elicited similar effects on cell viability and on induction of apoptosis, as
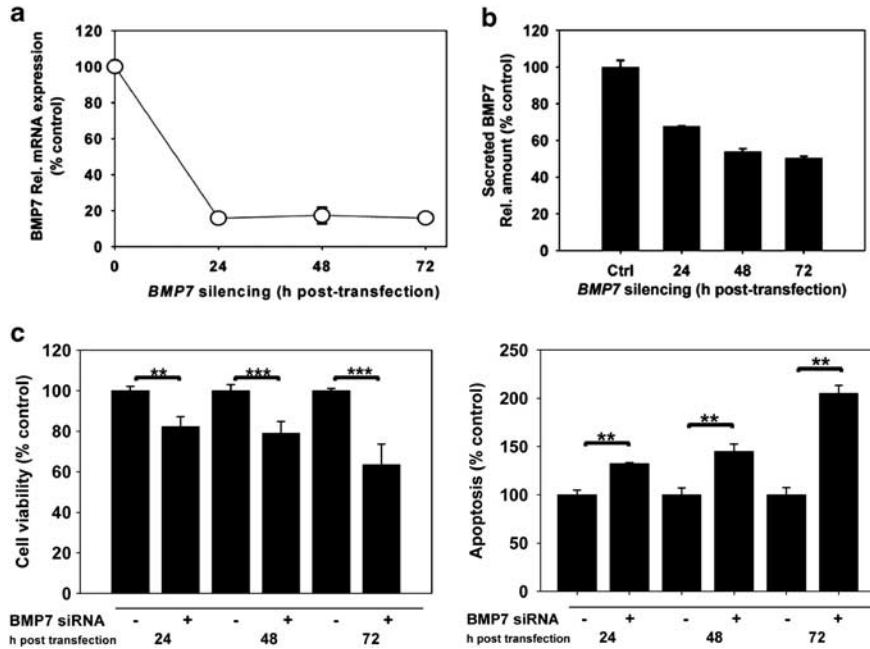
Figure 5 Effect of *BMP7* downregulation. (**a**) The mRNA expression level of *BMP7* in DAOY M2.1 cells is reported as the percentage of the *BMP7* level in control siRNA-transfected cells at the indicated time point. (**b**) Under the same conditions as in (**a**), the relative level of BMP7 secreted into the medium was evaluated by ELISA. (**c**) Cell viability and cell death induction were evaluated in DAOY M2.1 cells at the indicated time point after transfection with *MYC*-siRNA or control siRNA (**$P < 0.01$, ***$P < 0.001$ according to Student's *t*-test).

measured at 24–48 h after transfection, whereas silencing of *BMP6* alone was more effective after 72 h. Interestingly, the highest level of cell viability inhibition was achieved by the double knockdown (Supplementary Figure S4B), thus highlighting the relevant role of the BMP pathway for survival of MB cells.

To further study the effect of blocking the BMP/SMAD signaling pathway in MB cells, we also used dorsomorphin (DM), a small-molecule inhibitor of the BMP-dependent phosphorylation of the SMAD1/5/8 complex (Yu *et al.*, 2008). MB cells were assessed for cell viability in the presence of increasing concentrations of DM. Interestingly, cells overexpressing MYC were significantly more sensitive to DM than cells bearing one *MYC* copy (Figure 6a). In the same cell lines, phosphorylation of SMAD1/5/8 was prevented by DM, confirming the inhibitory effect of the compound on the pathway (Figure 6b). Furthermore, we found a dose-dependent effect of DM on cell proliferation (Figure 6c), even though no significant difference in induction of apoptosis was found in cells overexpressing MYC, if compared with wild type and empty-vector-transfected cells (Supplementary Figure S5A). On the contrary, DM induced a significantly stronger arrest of cell proliferation in cells expressing high MYC (Figure 6c). This observation suggested that DM can function as a cytotoxic agent inducing block of cell proliferation in a MYC-dependent way.

A panel of four distinct MB-derived cell lines expressing different levels of *BMP7* was additionally considered (Supplementary Figure S5B). The results showed that high *BMP7*-expressing cells (D425 and MED1) were more sensitive to DM than cells with lower *BMP7* levels (D341 and PFSK; Figure 6d). This

observation supported the presence of a BMP7-dependent mechanism sustaining cell survival, which DM is likely to target in MB cells.

Discussion

Owing to the key role in the development of MB, the oncogene *MYC* and MYC-target genes have become attractive therapeutic targets, in particular to treat the most aggressive MB subtypes (Grotzer *et al.*, 2009). With the aim of identifying MYC-driven genes or pathways with potentials as therapeutic target, we profiled MB-derived cells by cDNA microarray, following genetic manipulation for either overexpressing or downregulating *MYC*. The resulting sets of differentially expressed genes were intersected to narrow down the great amount of data generated, and thus to define a group of MYC-responsive genes. These genes included known direct targets, as well as novel candidate target genes of MYC. The gene ontology analysis on the data obtained, allowed identifying pathways that are known already to have a role in onset and progression of MB, but which had not been correlated yet with MYC expression. In particular, we found several components of the BMP/SMAD pathway, known to be physiologically active during embryogenesis, promoting cell proliferation and differentiation of precursor cells of the cerebellum, from which MB arises (Thompson *et al.*, 2006; Gilbertson and Ellison, 2008; Behesti and Marino, 2009; Sutter *et al.*, 2010). Several *in vivo* MB models confirmed that an unbalance of proliferative/differentiation signals, due to aberrant regulation of these pathways, can induce MB tumor formation
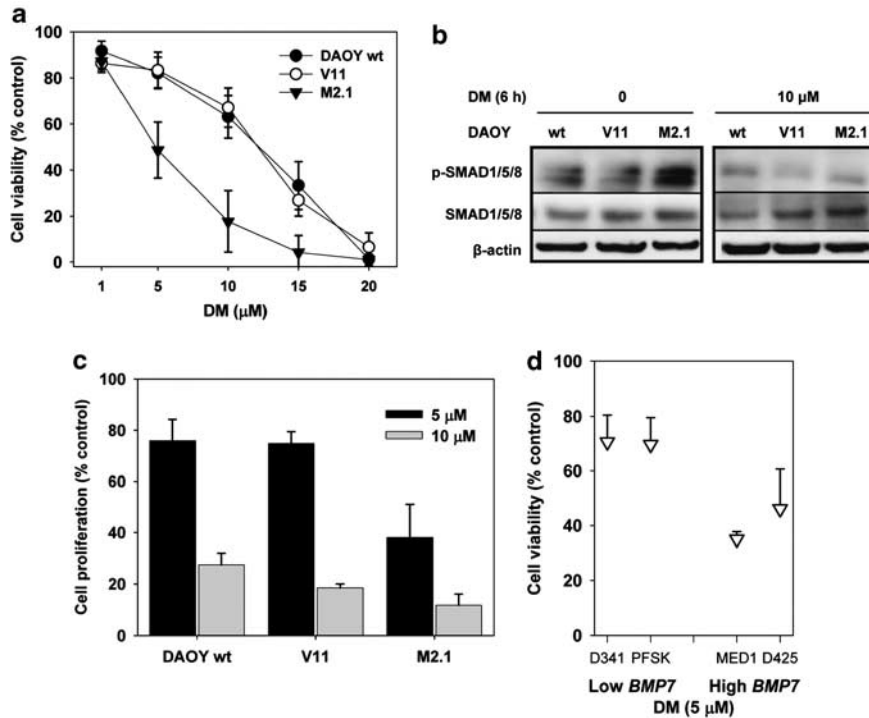
Figure 6 Inhibition of cell viability of MB cells by the BMP receptor kinase inhibitor dorsomorphin. (**a**) Cell viability was measured after 72 h of treatment with DM at the indicated concentrations. Results are expressed as the percentage of the values in vehicle-treated cells. (**b**) Phospho-SMAD1/5/8 and total SMAD1/5/8 content was investigated by western blot after treatment for 6 h with DM. (**c**) The effect of DM on cell proliferation was evaluated after 48 h. The reference was vehicle-treated cells. (**d**) The cellular response to DM was investigated in a panel of different MB-derived cell lines treated as in (**a**).

(Polkinghorn and Tarbell, 2007). In our study, *BMP7* was found consistently induced/repressed along with the up/downregulation of *MYC*, respectively, and thus chosen to be investigated in detail

Increasing evidences promote the role of the BMP/SMAD signaling pathway in determining the fate of the GNP cells of the cerebellum. In this context, components of this pathway and in particular BMP7 emerged and were further analyzed for a potential involvement in MYC-driven functions in MB. During the development of the cerebellum, BMP cytokines, including BMP7, are expressed by roof plate cells of the dorsal midline, a region adjacent to the rhombic lip (Alder *et al.*, 1999), and are known to coordinate proliferation and migration of GNPs (Chizhikov *et al.*, 2006). Members of the BMP family can in fact induce maturation of GNPs (Alder *et al.*, 1999) and survival of postnatal granule cells (Yabe *et al.*, 2002; Gilbertson and Ellison, 2008). BMP7 is constitutively expressed by cells of the choroid plexus of the forth ventricle, anatomically closed to the cerebellum (Dziegielewska *et al.*, 2001; Redzic and Segal, 2004), providing a pro-proliferative sustained signal for the GNP cells (Krizhanovsky and Ben-Arie, 2006; Grimmer and Weiss, 2008). Thus, determining the correct temporal/spatial organization of cerebellar progenitor cells during early development seems to be the main role of BMP7 (Thompson *et al.*, 2006). Along with this role, deregulated expression of BMP7 in the cerebellum is very likely associated with abnormal cell development and MB tumorigenesis.

As a validation of our *in vitro* results, BMP7 was analyzed by immunohistochemistry in primary MB samples. Strikingly, BMP7 was not expressed in normal cerebellum, indicating that overexpression of BMP7 in MB may contribute to the increased proliferation and survival of the tumor cells. Moreover, we found a significant correlation between the gene expression of *MYC* and *BMP7* in two distinct datasets of MB patient samples.

Further, we demonstrated that MYC can bind to the promoter of *BMP7* in different MB cell lines by using a ChIP-on-chip approach. That *BMP7* is a direct target of MYC was previously reported by Zeller *et al.* (2006) who performed a global mapping of MYC-binding genomic regions in a model of human B-lymphoid tumor. *BMP4*, another member of the same family, was described to be a target of MYC in blood cells (Fernandez *et al.*, 2003). These two reports represent the only experimental evidences, to our knowledge, about a transcriptional control of the BMP pathway by MYC, lacking however of functional information. More specifically, no previous studies have mentioned MYC-driven regulation of this pathway as a significant molecular network in MB.

This investigation, therefore, suggests for the first time the existence of a functional link between the overexpression of *MYC* and abnormal regulation of the BMP pathway in a model of MB. Furthermore, the functional relevance of the BMP-dependent signaling pathway in MB was evaluated by using DM,

a small-molecule inhibitor preventing the activation of SMAD1/5/8 by interfering with the kinase activity of the receptors BMPR-I/II (Anderson and Darshan, 2008; Yu et al., 2008). Conversely, DM has no, or very limited, effect on other components of the transforming growth factor-β family (fox example, transforming growth factor-β1 and activin A; Anderson and Darshan, 2008). We reported here the ability of DM to strongly impair proliferation and cell viability of MB-derived cells. More interestingly, cells expressing low MYC levels were significantly less sensitive to DM than cells overexpressing the oncogene, thus indicating that the compound can affect a MYC-driven pro-survival response. Moreover, silencing of *BMP7* induced cell death and inhibition of cell viability, although it was not as efficient as DM. This observation, however, is reasonable, because of the ability of the compound to block the pathway by interfering with more components at the same time.

Our results show the feasibility and potential benefit of a selective block of the BMP/SMAD pathway, by either silencing *BMP7* or using small-molecule inhibitors. A therapeutic approach interfering with activation of the BMP pathway was investigated here, for the first time, in MB cells and would represent one attractive strategy, to be considered in combination with targeting of sonic hedgehog and Wnt pathways (Chen et al., 2002; Romer and Curran, 2005; Luo et al., 2007; Rossi et al., 2008). Additional investigations on the role of other BMP family members will emphasize the relevance of the whole pathway in the development of MB. They will also help to shed lights on the emerging recent data showing opposite effects of BMPs, such as BMP2 and BMP4, to whom either anti-apoptotic (Iantosca et al., 1999) or anti-proliferative properties (Zhao et al., 2008) were assigned.

In conclusion, our results provide strong evidence of the induction of *BMP7* as a MYC-dependent mechanism and suggest BMP7 as an effector regulatory molecule, in the context of MYC-driven neoplastic transformation of MB precursor cells. This study, not only contributes to a better understanding of the prosurvival functions of MYC in MB, but it also suggests a rationale for targeting the BMP pathway in MB patients with *MYC* amplification/overexpression.

Materials and methods

MB cell lines
The human MB-derived DAOY, D341, D425, MED-1 and PFSK cell lines used in this study were obtained and maintained in culture as previously described (von Bueren et al., 2007). The stable clones DAOY V11 (empty vector transfected), DAOY M2.1 and DAOY M14 (*MYC* vector transfected) were maintained in selective medium in the presence of 500 ìg/ml G418 (Stearns et al., 2006).

RNA interference
The cells (70–80% confluent) were transfected using either SMARTpool siRNA specific for *MYC* or siCONTROL Non-targeting siRNA Pool as a control (Dharmacon, Thermo Fisher Scientific, Waltham, MA, USA). Each pool of siRNA was used at the final concentration of 50 nM in combination with Dharmafect 4 transfection reagent (Dharmacon), according to the manufacturer's instructions. Cells were harvested for both mRNA and protein extraction, to assess gene expression by quantitative real-time PCR and protein content by immunoblotting. To selectively target *BMP7* and other components of the BMP/SMAD pathway (*BMP2, BMP6* and BMP receptors *BMPR1A, BMPR1B, BMPR2, ACVR1, ACVR1B, ACVR1C, ACVR2A, ACVR2B* and *ACVRL1*), Ambion Silencer select predesigned siRNAs (Ambion Diagnostics, Applied Biosystems, Foster City, CA, USA) were used at 20 nM final concentration. As control, Silencer Negative Control siRNA #1 (cat. AM4611; Ambion Diagnostics) was used under the same conditions.

DNA microarray expression profiling and data analysis
The cDNA microarray analysis was performed in collaboration with the Functional Genomic Center of the University Zurich. Gene expression data were obtained by hybridizing Human Genome-U133 Plus 2.0 Affymetrix GeneChips arrays (Affymetrix, Santa Clara, CA, USA), on which >47 000 transcripts were represented. Raw data generated by the GCOS Software (Affymetrix) were processed by using the RMA method (Irizarry et al., 2003) and further statistically analyzed by using the software R and applying Student's t-test. Each experiment represented a group of three independent biological replicates. A gene was considered expressed only if the average normalized signal in at least one of the two groups compared was above 25. Results are expressed as fold change, and differences in expression were considered significant if fold change $\geqslant 2.0$ and P-value <0.01. The expression data were deposited in NCBI's Gene Expression Omnibus (Edgar et al., 2002) and are accessible through GEO series accession number GSE22139 (http://www.ncbi.nlm.nih.gov/geo). Cluster analysis of the data was performed by using the heatmap.2 method of the 'gplots' package (R Development Core Team, 2008). The GeneGO MetaCore (GeneGO, St Joseph, MI, USA) was used to define functional annotations for the selected genes, thus assigning them to ontological categories for association with relevant biological processes and pathways.

MB TMA and BMP7/MYC correlation study in MB patient samples
The tumor material used to create the MB TMA originates from three sets of archival MB samples, diagnosed in Zurich, Switzerland ($n = 46$), Cairo, Egypt ($n = 14$) and Tübingen, Germany ($n = 6$). All these tumor samples were reviewed independently by two neuropathologists and diagnosed as MB.

TMA paraffin sections were deparaffinized in xylene and rehydrated stepwise with ethanol. The immunohistochemistry determination of BMP7 was carried out using the catalyzed signal amplification II system (Dako, Glostrup, Denmark) according to the manufacturer's protocol. The endogenous peroxidase activity was blocked incubating the specimens with 0.3% H_2O_2 for 5 min, followed by 5 min with a protein-based blocking reagent and incubation with a BMP7-specific antibody (Abcam, Cambridge, UK; 1:3000), for 30 min at room temperature. The signal was detected in the presence of diaminobenzidine. Immunoreactivity was scored as (i) −, if <10%; (ii) +, if 10–50%; (iii) + +, if 51–90%; (iv) + + +, if >90% of neoplastic cells with cytoplasmic staining for BMP7. Human normal kidney tissues on paraffin sections served as a positive control. From a subset of 38 samples from

the MB patients diagnosed in Zurich (Switzerland) sufficient tumor material was available to perform quantitative real-time PCR for the analysis of *BMP7* and *MYC* mRNA expression. Total RNA was isolated from formalin-fixed paraffin-embedded tumor tissue as described previously (Kunz *et al.*, 2006) by using the Optimum formalin-fixed paraffin-embedded for paraffin block RNA isolation kit (Ambion Diagnostics). Paraffin from 1×20 to $2 \times 20 \, \mu m$ slices of formalin-fixed paraffin-embedded MB samples was removed by washing the samples with xylene for 30 min. Samples were collected by centrifugation, washed with ethanol,and allowed to air dry at room temperature prior final centrifugation. Samples were then resuspended in $10 \, \mu l$ ($60 \, U/\mu l$) proteinase K and $100 \, \mu l$ of digestion buffer, and incubated at $37^\circ C$ for 3 h and then at room temperature for further 12 h. After complete digestion, RNA was extracted according to the manufacturer's protocol.

To validate our results, expression data obtained from a different group of primary MB tumors (Thompson *et al.*, 2006) was used to perform an unsupervised analysis on the mRNA expression of *BMP7* and *MYC*.

Cell viability, cell proliferation and apoptosis assays
Cell viability was evaluated using the CellTiter 96 AQ$_{ueous}$ One Solution Cell Proliferation Assay (Promega Corporation, Madison, WI, USA) based on the reactivity of (3-(4,5-dimethylthiazol-2-yl)-5-(3-carboxymethoxyphenyl)-2-(4-sulfophenyl)-2H-tetrazolium). Alternatively, the number of viable cells was determined by trypan blue exclusion using a hemocytometer. Proliferation was quantified by the chemiluminescence-based Cell Proliferation ELISA BrdU (F Hoffmann-La Roche AG, Basel Switzerland). Activation of caspases 3 and 7 was detected by using the Caspase-Glo 3/7 Assay (Promega Corporation); histone-associated DNA fragments were quantified by Cell Death Detection ELISA^{PLUS} assay (Roche Diagnostics). Data are expressed as average values from three independent experiments.

Gene expression analysis
Total RNA was extracted using the RNeasy Mini Kit (Qiagen, Basel, Switzerland) following the manufacturer's instructions. After enzymatic digestion of DNA with RNase-free DNase (Qiagen), $0.5–1 \, \mu g$ of total RNA was used as template for reverse transcription, which was triggered by random hexamer primers and performed by using the High-Capacity cDNA Reverse Transcription Kit (Applied Biosystems). Quantitative real-time PCR was performed under conditions optimized for the ABI7900HT instrument, using Gene Expression Master Mix (Applied Biosystems). Probe-primer specific for the following genes (purchased from Applied Biosystems) were used: *MYC* (Hs00153408_m1), *BMP7* (Hs00233476_m1), *TERT* (Hs00162669_m1), *CCND2* (Hs00277041_m1) and *CCNA2* (Hs00153138_m1). Normal human cerebellum was used as a reference (Clontech-Takara Bio Europe, Saint-Germain-en-Laye, France). The relative gene expression was

calculated for each gene of interest by using the $\Delta\Delta C_T$ method, where cycle threshold (C_T) values were normalized to the housekeeping genes succinate dehydrogenase complex subunit A (*SDHA*) (Hs00188166_m1) and β-actin (Hs99999903_m1).

Western blot analysis and ELISA
Total protein extracts were obtained from $0.5–1.5 \times 10^6$ cells lysed with RIPA buffer (50 mM Tris-Cl, pH 6.8, 100 mM NaCl, 1% Triton X-100, 0.1% SDS) supplemented with Complete Mini Protease Inhibitor Cocktail (Roche Applied Sciences) and with the phosphatase inhibitors β-glycerophosphate (20 mM) and Na_3VO_4 (200 μM). Proteins were resolved by SDS–polyacrylamide gel electrophoresis and western blotting on polyvinylidene fluoride membranes (Amersham, GE Healthcare, UK). After binding of the indicated antibodies, the signal was detected by chemiluminescence using SuperSignal West Femto Maximum Sensitivity Substrate (Thermo Fisher Scientific Inc., Rockford, IL, USA). Antibodies specific for BMP7 (4E7) and SMAD 1/5/8 (N-18) were purchased from Santa Cruz Biotechnology Inc., whereas antibodies against phospho-SMAD1 (Ser463/465), SMAD5 (Ser463/465), SMAD8 (Ser426/428) and MYC were from Cell Signaling Technology, Inc. (Danvers, MA, USA). As loading controls, β-tubulin and β-actin (Sigma-Aldrich Chemie GmbH, Buchs, Germany) were detected. According to the experimental setting, cells were incubated in the presence of human recombinant BMP7 (Calbiochem-Merck, Darmstadt, Germany) for 0.5 or 1 h, and cell lysates were analyzed by western blotting. To quantify secreted BMP7 in cell supernatants (100 μl from each sample), the human BMP7 ELISA kit (RayBiotech Inc., Norcross, GA, USA) was used following the manufacturers' instructions.

ChIP-on-chip
ChIP-on-chip experiments using a MYC antibody were performed as previously described (Ma *et al.*, 2010). The MB-derived cell lines D487 and D283 were used in this study.

Statistical analysis
All experiments were performed at least in triplicates. Data are represented as mean ± s.d. For *in vitro* experiments, the Student's *t*-test was used. *P*-values of <0.01 were considered significant. Pearson's correlation test and Fisher's exact test were used for *in vivo* gene correlation.

Conflict of interest

The authors declare no conflict of interest.

Acknowledgements

References

Adhikary S, Eilers M. (2005). Transcriptional regulation and transformation by Myc proteins. *Nat Rev Mol Cell Biol* **6**: 635–645.

Alder J, Lee KJ, Jessell TM, Hatten ME. (1999). Generation of cerebellar granule neurons in vivo by transplantation of BMP-treated neural progenitor cells. *Nat Neurosci* **2**: 535–540.

Aldosari N, Bigner SH, Burger PC, Becker L, Kepner JL, Friedman HS *et al.* (2002). MYCC and MYCN oncogene amplification in medulloblastoma. A fluorescence in situ hybridization study on paraffin sections from the Children's Oncology Group. *Arch Pathol Lab Med* **126**: 540–544.

Anderson GJ, Darshan D. (2008). Small-molecule dissection of BMP signaling. *Nat Chem Biol* **4**: 15–16.

Arihiro K, Inai K. (2001). Expression of CD31, Met/hepatocyte growth factor receptor and bone morphogenetic protein in bone metastasis of osteosarcoma. *Pathol Int* **51**: 100–106.

Balemans W, Van Hul W. (2002). Extracellular regulation of BMP signaling in vertebrates: a cocktail of modulators. *Dev Biol* **250**: 231–250.

Behesti H, Marino S. (2009). Cerebellar granule cells: insights into proliferation, differentiation, and role in medulloblastoma pathogenesis. *Int J Biochem Cell Biol* **41**: 435–445.

Blanco Calvo M, Bolos Fernandez V, Medina Villaamil V, Aparicio Gallego G, Diaz Prado S, Grande Pulido E. (2009). Biology of BMP signalling and cancer. *Clin Transl Oncol* **11**: 126–137.

Buijs JT, Henriquez NV, van Overveld PG, van der Horst G, Que I, Schwaninger R *et al*. (2007a). Bone morphogenetic protein 7 in the development and treatment of bone metastases from breast cancer. *Cancer Res* **67**: 8742–8751.

Buijs JT, Petersen M, van der Horst G, van der Pluijm G. (2010). Bone morphogenetic proteins and its receptors; therapeutic targets in cancer progression and bone metastasis? *Curr Pharm Des* **16**: 1291–1300.

Buijs JT, Rentsch CA, van der Horst G, van Overveld PG, Wetterwald A, Schwaninger R *et al*. (2007b). BMP7, a putative regulator of epithelial homeostasis in the human prostate, is a potent inhibitor of prostate cancer bone metastasis in vivo. *Am J Pathol* **171**: 1047–1057.

Chen JK, Taipale J, Cooper MK, Beachy PA. (2002). Inhibition of Hedgehog signaling by direct binding of cyclopamine to smoothened. *Genes Dev* **16**: 2743–2748.

Chizhikov VV, Lindgren AG, Currle DS, Rose MF, Monuki ES, Millen KJ. (2006). The roof plate regulates cerebellar cell-type specification and proliferation. *Development* **133**: 2793–2804.

Crawford JR, MacDonald TJ, Packer RJ. (2007). Medulloblastoma in childhood: new biological advances. *Lancet Neurol* **6**: 1073–1085.

Dai J, Hall CL, Escara-Wilke J, Mizokami A, Keller JM, Keller ET. (2008). Prostate cancer induces bone metastasis through Wnt-induced bone morphogenetic protein-dependent and independent mechanisms. *Cancer Res* **68**: 5785–5794.

Derynck R, Akhurst RJ, Balmain A. (2001). TGF-beta signaling in tumor suppression and cancer progression. *Nat Genet* **29**: 117–129.

Dziegielewska KM, Ek J, Habgood MD, Saunders NR. (2001). Development of the choroid plexus. *Microsc Res Tech* **52**: 5–20.

Eberhart CG, Kepner JL, Goldthwaite PT, Kun LE, Duffner PK, Friedman HS *et al*. (2002). Histopathologic grading of medulloblastomas: a Pediatric Oncology Group study. *Cancer* **94**: 552–560.

Edgar R, Domrachev M, Lash AE. (2002). Gene expression omnibus: NCBI gene expression and hybridization array data repository. *Nucleic Acids Res* **30**: 207–210.

Engelhard HH, Corsten LA. (2005). Leptomeningeal metastasis of primary central nervous system (CNS) neoplasms. *Cancer Treat Res* **125**: 71–85.

Feeley BT, Gamradt SC, Hsu WK, Liu N, Krenek L, Robbins P *et al*. (2005). Influence of BMPs on the formation of osteoblastic lesions in metastatic prostate cancer. *J Bone Miner Res* **20**: 2189–2199.

Fernandez PC, Frank SR, Wang L, Schroeder M, Liu S, Greene J *et al*. (2003). Genomic targets of the human c-Myc protein. *Genes Dev* **17**: 1115–1129.

Filmus J, Capurro M, Rast J. (2008). Glypicans. *Genome Biol* **9**: 224.

Gilbertson RJ, Ellison DW. (2008). The origins of medulloblastoma subtypes. *Annu Rev Pathol* **3**: 341–365.

Grandori C, Cowley SM, James LP, Eisenman RN. (2000). The Myc/Max/Mad network and the transcriptional control of cell behavior. *Annu Rev Cell Dev Biol* **16**: 653–699.

Grimmer MR, Weiss WA. (2008). BMPs oppose Math1 in cerebellar development and in medulloblastoma. *Genes Dev* **22**: 693–699.

Grisaru S, Cano-Gauci D, Tee J, Filmus J, Rosenblum ND. (2001). Glypican-3 modulates BMP- and FGF-mediated effects during renal branching morphogenesis. *Dev Biol* **231**: 31–46.

Grotzer MA, Castelletti D, Fiaschetti G, Shalaby T, Arcaro A. (2009). Targeting Myc in pediatric malignancies of the central and peripheral nervous system. *Curr Cancer Drug Targets* **9**: 176–188.

Guessous F, Li Y, Abounader R. (2008). Signaling pathways in medulloblastoma. *J Cell Physiol* **217**: 577–583.

Guhaniyogi J, Brewer G. (2001). Regulation of mRNA stability in mammalian cells. *Gene* **265**: 11–23.

Guo X, Wang XF. (2009). Signaling cross-talk between TGF-beta/BMP and other pathways. *Cell Res* **19**: 71–88.

Gurney JG, Kadan-Lottick N. (2001). Brain and other central nervous system tumors: rates, trends, and epidemiology. *Curr Opin Oncol* **13**: 160–166.

Herms J, Neidt I, Luscher B, Sommer A, Schurmann P, Schroder T *et al*. (2000). C-MYC expression in medulloblastoma and its prognostic value. *Int J Cancer* **89**: 395–402.

Iantosca MR, McPherson CE, Ho SY, Maxwell GD. (1999). Bone morphogenetic proteins-2 and -4 attenuate apoptosis in a cerebellar primitive neuroectodermal tumor cell line. *J Neurosci Res* **56**: 248–258.

Irizarry RA, Bolstad BM, Collin F, Cope LM, Hobbs B, Speed TP. (2003). Summaries of Affymetrix GeneChip probe level data. *Nucleic Acids Res* **31**: e15.

Krizhanovsky V, Ben-Arie N. (2006). A novel role for the choroid plexus in BMP-mediated inhibition of differentiation of cerebellar neural progenitors. *Mech Dev* **123**: 67–75.

Kunz F, Shalaby T, Lang D, von Buren A, Hainfellner JA, Slavc I *et al*. (2006). Quantitative mRNA expression analysis of neurotrophin-receptor TrkC and oncogene c-MYC from formalin-fixed, paraffin-embedded primitive neuroectodermal tumor samples. *Neuropathology* **26**: 393–399.

Lamont JM, McManamy CS, Pearson AD, Clifford SC, Ellison DW. (2004). Combined histopathological and molecular cytogenetic stratification of medulloblastoma patients. *Clin Cancer Res* **10**: 5482–5493.

Langenfeld EM, Calvano SE, Abou-Nukta F, Lowry SF, Amenta P, Langenfeld J. (2003). The mature bone morphogenetic protein-2 is aberrantly expressed in non-small cell lung carcinomas and stimulates tumor growth of A549 cells. *Carcinogenesis* **24**: 1445–1454.

Littlewood TD, Evan GI. (1990). The role of myc oncogenes in cell growth and differentiation. *Adv Dent Res* **4**: 69–79.

Luo J, Chen J, Deng ZL, Luo X, Song WX, Sharff KA *et al*. (2007). Wnt signaling and human diseases: what are the therapeutic implications? *Lab Invest* **87**: 97–103.

Ma L, Young J, Prabhala H, Pan E, Mestdagh P, Muth D *et al*. (2010). miR-9, a MYC/MYCN-activated microRNA, regulates E-cadherin and cancer metastasis. *Nat Cell Biol* **12**: 247–256.

Marino S. (2005). Medulloblastoma: developmental mechanisms out of control. *Trends Mol Med* **11**: 17–22.

Miyazaki H, Watabe T, Kitamura T, Miyazono K. (2004). BMP signals inhibit proliferation and in vivo tumor growth of androgen-insensitive prostate carcinoma cells. *Oncogene* **23**: 9326–9335.

Miyazono K. (1999). Signal transduction by bone morphogenetic protein receptors: functional roles of Smad proteins. *Bone* **25**: 91–93.

Miyazono K, Kamiya Y, Morikawa M. (2010). Bone morphogenetic protein receptors and signal transduction. *J Biochem* **147**: 35–51.

Miyazono K, Maeda S, Imamura T. (2005). BMP receptor signaling: transcriptional targets, regulation of signals, and signaling cross-talk. *Cytokine Growth Factor Rev* **16**: 251–263.

Mulhern RK, Palmer SL, Merchant TE, Wallace D, Kocak M, Brouwers P *et al*. (2005). Neurocognitive consequences of risk-adapted therapy for childhood medulloblastoma. *J Clin Oncol* **23**: 5511–5519.

Neben K, Korshunov A, Benner A, Wrobel G, Hahn M, Kokocinski F *et al*. (2004). Microarray-based screening for molecular markers in medulloblastoma revealed STK15 as independent predictor for survival. *Cancer Res* **64**: 3103–3111.

Piccirillo SG, Vescovi AL. (2006). Bone morphogenetic proteins regulate tumorigenicity in human glioblastoma stem cells. *Ernst Schering Found Symp Proc* **5**: 59–81.

Polkinghorn WR, Tarbell NJ. (2007). Medulloblastoma: tumorigenesis, current clinical paradigm, and efforts to improve risk stratification. *Nat Clin Pract Oncol* **4**: 295–304.

Raida M, Clement JH, Ameri K, Han C, Leek RD, Harris AL. (2005). Expression of bone morphogenetic protein 2 in breast cancer cells inhibits hypoxic cell death. *Int J Oncol* **26**: 1465–1470.

Redzic ZB, Segal MB. (2004). The structure of the choroid plexus and the physiology of the choroid plexus epithelium. *Adv Drug Deliv Rev* **56**: 1695–1716.

Romer J, Curran T. (2005). Targeting medulloblastoma: small-molecule inhibitors of the Sonic Hedgehog pathway as potential cancer therapeutics. *Cancer Res* **65**: 4975–4978.

Rossi A, Caracciolo V, Russo G, Reiss K, Giordano A. (2008). Medulloblastoma: from molecular pathology to therapy. *Clin Cancer Res* **14**: 971–976.

Sieber C, Kopf J, Hiepen C, Knaus P. (2009). Recent advances in BMP receptor signaling. *Cytokine Growth Factor Rev* **20**: 343–355.

Stearns D, Chaudhry A, Abel TW, Burger PC, Dang CV, Eberhart CG. (2006). c-Myc overexpression causes anaplasia in medulloblastoma. *Cancer Res* **66**: 673–681.

Sutter R, Shakhova O, Bhagat H, Behesti H, Sutter C, Penkar S *et al*. (2010). Cerebellar stem cells act as medulloblastoma-initiating cells in a mouse model and a neural stem cell signature characterizes a subset of human medulloblastomas. *Oncogene* **29**: 1845–1856.

Thawani JP, Wang AC, Than KD, Lin CY, La Marca F, Park P. (2010). Bone morphogenetic proteins and cancer: review of the literature. *Neurosurgery* **66**: 233–246; discussion 246.

Thompson MC, Fuller C, Hogg TL, Dalton J, Finkelstein D, Lau CC *et al*. (2006). Genomics identifies medulloblastoma subgroups that are enriched for specific genetic alterations. *J Clin Oncol* **24**: 1924–1931.

Vita M, Henriksson M. (2006). The Myc oncoprotein as a therapeutic target for human cancer. *Semin Cancer Biol* **16**: 318–330.

von Bueren AO, Shalaby T, Rajtarova J, Stearns D, Eberhart CG, Helson L *et al*. (2007). Anti-proliferative activity of the quassinoid NBT-272 in childhood medulloblastoma cells. *BMC Cancer* **7**: 19.

Walsh DW, Godson C, Brazil DP, Martin F. (2010). Extracellular BMP-antagonist regulation in development and disease: tied up in knots. *Trends Cell Biol* **20**: 244–256.

Wu KJ, Grandori C, Amacker M, Simon-Vermot N, Polack A, Lingner J *et al*. (1999). Direct activation of TERT transcription by c-MYC. *Nat Genet* **21**: 220–224.

Yabe T, Samuels I, Schwartz JP. (2002). Bone morphogenetic proteins BMP-6 and BMP-7 have differential effects on survival and neurite outgrowth of cerebellar granule cell neurons. *J Neurosci Res* **68**: 161–168.

Yan W, Chen X. (2007). Targeted repression of bone morphogenetic protein 7, a novel target of the p53 family, triggers proliferative defect in p53-deficient breast cancer cells. *Cancer Res* **67**: 9117–9124.

Yanagita M. (2005). BMP antagonists: their roles in development and involvement in pathophysiology. *Cytokine Growth Factor Rev* **16**: 309–317.

Yanagita M. (2009). BMP modulators regulate the function of BMP during body patterning and disease progression. *Biofactors* **35**: 113–119.

Ye L, Bokobza SM, Jiang WG. (2009). Bone morphogenetic proteins in development and progression of breast cancer and therapeutic potential (review). *Int J Mol Med* **24**: 591–597.

Ye L, Lewis-Russell JM, Davies G, Sanders AJ, Kynaston H, Jiang WG. (2007). Hepatocyte growth factor up-regulates the expression of the bone morphogenetic protein (BMP) receptors, BMPR-IB and BMPR-II, in human prostate cancer cells. *Int J Oncol* **30**: 521–529.

Yu PB, Hong CC, Sachidanandan C, Babitt JL, Deng DY, Hoyng SA *et al*. (2008). Dorsomorphin inhibits BMP signals required for embryogenesis and iron metabolism. *Nat Chem Biol* **4**: 33–41.

Zeller KI, Zhao X, Lee CW, Chiu KP, Yao F, Yustein JT *et al*. (2006). Global mapping of c-Myc binding sites and target gene networks in human B cells. *Proc Natl Acad Sci USA* **103**: 17834–17839.

Zhao H, Ayrault O, Zindy F, Kim JH, Roussel MF. (2008). Post-transcriptional down-regulation of Atoh1/Math1 by bone morphogenic proteins suppresses medulloblastoma development. *Genes Dev* **22**: 722–727.

Supplementary Information accompanies the paper on the Oncogene website (http://www.nature.com/onc)